Quantum Electronics **30** (7) 635 – 640 (2000)

LASER APPLICATIONS AND OTHER TOPICS IN QUANTUM ELECTRONICS

PACS numbers: 42.70.Df; 42.70.Ln; 42.70.Ht
DOI: 10.1070/QE2000v030n07ABEH001781

Holographic recording in films of azo-containing LC polymers in the presence of orienting electric field

A N Simonov, A V Larichev, V P Shibaev

Abstract. The dynamics of holographic recording in a film of azo-containing liquid-crystal polymer is studied both experimentally and theoretically in the presence of the orienting electric field. The possibility is demonstrated to efficiently control the optical recording regime by varying the applied field. The specificity of hologram formation in the case of different polarisation of the interacting light beams is considered. A theoretical model describing the holographic recording dynamics in a film of azo-containing nematic polymer is presented; numerical simulation of the processes of recording and read-out in anisotropic holograms is carried out as well.

1. Introduction

The capability to control the diffractional characteristics of the photosensitive media manifesting liquid-crystal (LC) properties is of great interest for optical data processing and storage. Sutherland et al. [1 – 3] considered the possibilities for realising this control during the read-out of pre-recorded holograms. However, in photochromic polymer LC materials containing azo-dye fragments, the holographic properties of the media can be controlled directly at the recording stage by using an orienting electric field [4, 5]. This is related to the fact that anisotropic chromophores participating in the formation of the LC mesophase are mostly oriented along the LC director of the polymer. When an electric field is applied, the LC director reorients itself in the layer, changing the efficiency of the interaction between the azo dye and the light. This finally leads to a variation in the light-induced term of the refractive index $\Delta n_{\rm ind}$ and a modification of the optical recording depth in the polymer sample [5].

Birefringent organic compounds containing azo dyes can be used for highly efficient recording of anisotropic (polarisation) holograms [6 – 8]. Of particular interest for the applications are the holographic recording processes based on intermodal diffraction, since they permit a significant increase in the signal-to-noise ratio during the read-out of optical data and realisation of wide-band data reproduction [9]. The fact that photoanisotropic properties of azo-containing LC polymers depend on the applied electric field makes these materials attractive for controlled selective read-out of the optical data recorded as volume holograms.

In this work, we studied experimentally and theoretically the holographic recording dynamics in a film of azo-containing nematic LC polymer with cyanobiphenyl fragments [10, 11]. We consider the influence of the orienting electric field on the efficiency of diffractional processes.

To the best of our knowledge, the dynamics of the processes of read-out and recording of anisotropic holograms in azo-containing LC polymers has not been studied experimentally and theoretically so far. Huang et al. [8] analysed the stationary regime of holographic recording in amorphous azo-containing materials using rather strong simplifying assumptions.

2. Statement of the problem. The computational model

Consider the process of simultaneous hologram recording and read-out in a film of photosensitive azo-containing LC polymer for the geometry shown in Figs 1 a,d. The polymer layer of thickness L is illuminated by two recording light beams ($\boldsymbol{E}_1$ and $\boldsymbol{E}_2$ are the electric field vectors of the light waves) of either parallel (s – s, Fig. 1a) or orthogonal (s – p, Fig. 1d) polarisation. The hologram is read out by the s-polarised probe beam $\boldsymbol{E}_{\rm p}$ at the wavelength $\lambda_{\rm p}$ ($\lambda_{\rm p} > \lambda_{\rm r}$, where $\lambda_{\rm r}$ is the corresponding wavelength in vacuum); the probe beam propagates at the Bragg angle with respect to the film. The applied electric field $\boldsymbol{E}_{\rm a}$ determines the orientation of the polymer layer.

Illumination of the polymer by the beams $\boldsymbol{E}_1$, $\boldsymbol{E}_2$ leads to the formation of the dynamic anisotropic gratings of the refractive index $\Delta\hat{n}(z, x, t)$ and the intensity-transmission coefficient $\hat{T}(z, x, t)$; this gratings scatter both the probe beam and the recording beams. The form of the tensor functions $\Delta\hat{n}(z, x, t)$, $\Delta\hat{T}(z, x, t)$ is determined by the polarisation and the propagation directions of the recording light beams (i. e., the type of the diffractional process). Due to nonlinear light absorption inside the polymer, the grating amplitudes depend on the depth (along the axis Z) in rather complicated ways. In the general case, the analytical calculation of the processes of recording and read-out of anisotropic dynamic holograms in a polymer layer of a finite thickness is not feasible; for these reasons, the following theoretical analysis will be based on the numerical simulation methods.

We represent the polymer film as a set of amplitude-phase screens that are arranged along the Z-axis with the spacing Δz, and introduce the following notation for the light fields

$$\boldsymbol{E}_i = \boldsymbol{e}_i E_i, \quad E_i = \frac{1}{2} A_i(z, x) \exp(\mathrm{i}\boldsymbol{k}_i \boldsymbol{r}) + \text{c.c.} \tag{1}$$

A N Simonov, A V Larichev International Teaching and Research Laser Centre at the M V Lomonosov Moscow State University, Vorob'yovy Gory, 119899 Moscow, Russia
V P Shibaev Chemistry Department, M V Lomonosov Moscow State University, Vorob'yovy Gory, 119899 Moscow, Russia

Received 30 December 1999
Kvantovaya Elektronika **30** (7) 635 – 640 (2000)
Translated by I V Bargatin, edited by M N Sapozhnikov

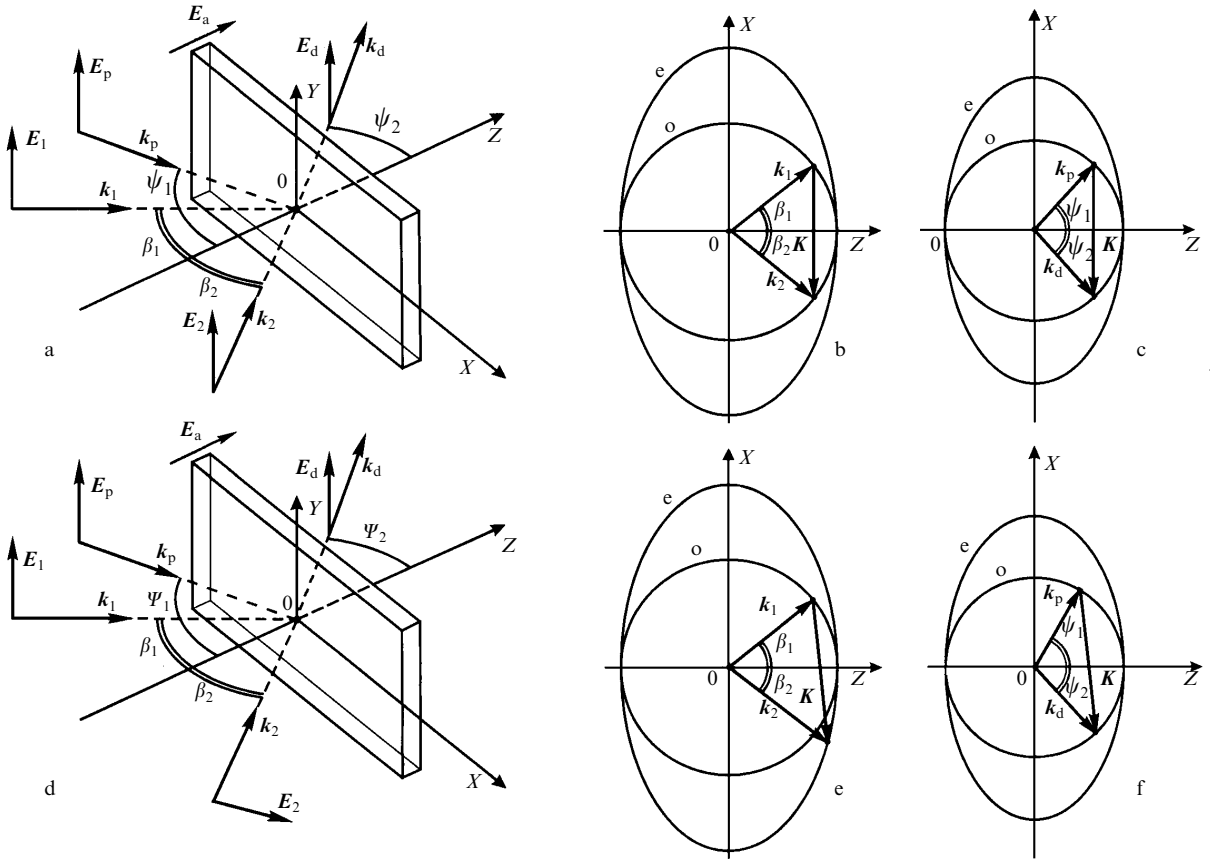

Figure 1. The geometry of holographic recording by s – s-polarised (a) and s – p-polarised (d) laser beams, and the vector diagrams of the corresponding diffractional processes in the oriented LC polymer film: the intramodal (b) and intermodal (e) recording, and the intramodal read-out of the holograms (c and (f)).

where $A_i(z,x)$ is the complex amplitude; $\boldsymbol{e}_i$ is the unit vector of polarisation; and $\boldsymbol{k}_i$ is the wave vector of the light beam ($i=1,2$ corresponds to the recording beams; $i=\mathrm{p}$ to the probe beam). The wave number of the beams in the anisotropic medium is given by $k_i = 2n_i/\lambda_i$, where the index of refraction n_i is determined by the polarisation and the propagation direction of the ith beam. Assuming that the complex amplitudes $A_i(z,x)$ in the plane z are known, we will calculate the field amplitudes in the next layer $z+\Delta z$. The resulting calculation procedure will then be extended to the entire film thickness L. The sequence of the computational steps can be represented as follows:

(1) Using the photoprocess equations for the polymer and the given amplitudes $A_1(z,x)$ and $A_2(z,x)$, we calculate the parameters $\Delta\hat{n}(z,x,t)$ and $\hat{T}(z,x,t)$ of the anisotropic amplitude-phase screen.

(2) Using the explicit form of $\Delta\hat{n}(z,x,t)$ and $\hat{T}(z,x,t)$, we consider the diffraction of the recording light beams:

$$A_i(z+\Delta z,x) = \hat{P}(\Delta z)[T(z,x,t)]^{1/2}A_i(z,x)$$
$$\times \exp[\mathrm{i}k_i\Delta n(z,x,t)\Delta z/\bar{n}].$$

Here, $\hat{P}(\Delta z)$ is the operator of propagation (diffraction) over the distance Δz; $\Delta n(z,x,t)$ is the addition to the refractive index due to the considered diffractional process; $i=1,2$; and n is the unperturbed value of the refractive index.

(3) We assume that the probe beam does not induce phototransformations in the polymer and neglect the scattering of the probe beam by the amplitude component of the recorded grating. Taking into account the calculated phase inhomogeneity of the layer, we find

$$A_\mathrm{p}(z+\Delta z,x) = \hat{P}(\Delta z)A_\mathrm{p}(z,x)$$
$$\times \exp[\mathrm{i}k_\mathrm{p}\Delta n(z,x,t)\Delta z/\bar{n} - \kappa_\mathrm{p}\Delta z/2],$$

where kp is the intensity absorption coefficient of the probe beam.

Therefore, the main computational steps are reduced to finding the parameters of the model amplitude-phase screen for the current polymer layer and calculating the diffraction of the light beams from each intermediate layer.

Figs 1 b, c and 1 e, f show the diagrams of the diffractional processes that correspond to the interaction geometry shown, in Figs 1 a and 1 d, respectively. These figures show the cross sections of the surfaces formed by the wave vectors of the ordinary (o-) wave (s-polarisation) and the extraordinary (e-) wave (p-polarisation) for the processes of the hologram recording and read-out. The recording and the read-out shown respectively in Figs 1 b and 1 c are performed by ordinary s-polarised beams using the intramodal diffraction without change of polarisation. At the same time, the recording shown in Fig. 1 e is the intermodal process using s – p-polarised beams, while the read-out shown in Fig. 1 f is the intramodal process using s – s-polarised beams.

Using the presented diagrams and the identity of the grating vectors $\boldsymbol{K}$ corresponding to the recording and the read-out processes, we can determine the read-out angle ψ_1 and the diffraction angle ψ_2 that satisfy the Bragg condition for the probe light beam (all angles here refer to propagation direction inside the polymer). For instance, for the geometry shown in Fig. 1a, we easily find

$$\psi_1 = \psi_2 = \arcsin\left(\frac{\lambda_p}{\lambda_r}\sin\beta_1\right). \quad (2)$$

Here, we take into account that $\beta_1 = \beta_2$ in experiments. In the case of intermodal diffraction (Fig. 1 d), we can determine the angles ψ_1 and ψ_2 by equating the X- and Z-components of the grating vector $\boldsymbol{K}$ for the processes of the hologram recording (Fig. 1 e) and read-out (Fig. 1 f). Using the condition $\beta_1 = \beta_2$, we obtain

$$\sin\beta_1[n_e(\beta_1) + n_\perp]\lambda_p = n_\perp(\sin\psi_1 + \sin\psi_2)\lambda_r,$$
$$\cos\beta_1[n_e(\beta_1) - n_\perp]\lambda_p = n_\perp(\cos\psi_2 - \cos\psi_1)\lambda_r. \quad (3)$$

where $n_e(\beta_1) = \left(\cos^2\beta_1/n_\perp^2 + \sin^2\beta_1/n_\parallel^2\right)^{-1/2}$ is the refractive index for the extraordinary wave propagating at the angle β_1; $n_\parallel, n_\perp$ are the principal values of the refractive index of the aligned polymer film in the longitudinal and transverse directions with respect to the LC director.

The derived expressions (2) and (3) will be later used in the numerical simulation to determine the angles ψ_1 and ψ_2 of propagation of the probe beam inside the polymer that satisfy the Bragg condition. Note that the splitting of the wave-vector surfaces due to birefringence, $\sim 2\pi(n_\parallel - n_\perp)/\lambda_p$, exceeds the indeterminacy of the wave vector due to the finite hologram thickness, $\sim 2\pi/d$, where $d = \min(L, d_{ef})$, and d_{ef} – is effective depth of the hologram recording. As a result, different diffraction types are resolved with respect to the angle. The strict fixation of the polarisation and the angles of incidence of the light beams thus uniquely defines the type of the diffractional process.

We will analyse the diffraction of the light beams using the beam propagating method (BPM) (see, e.g., [12]). For a known complex field amplitude $A(z, x)$ in the layer z, this method allows one to calculate the field amplitude $A(z+\Delta z, x)$ in the next layer $z + \Delta z$ corresponding to diffraction in a homogeneous medium:

$$A(z+\Delta z, x) = \hat{P}(\Delta z)A(z,x) = \hat{F}^{-1}\{\hat{F}[A(z,x'), x'; k_x]$$
$$\times \exp\left[i\Delta z\left(\sqrt{k^2 - k_x^2} - k\right)\right], k_x; x\}. \quad (4)$$

Here, k is the wave number; $\hat{F}[\,]$, $\hat{F}^{-1}\{\,\}$ are the operators of the forward and the backward Fourier transforms. Note that, in contrast to the usual paraxial BPM, algorithm (4) is the exact solution of the scalar Helmholtz equation for the TE wave. Using this approach, we can adequately account for the diffraction of the light beams propagating at large angles with respect to the normal to the layer. A similar expression for the amplitude of the magnetic field of the light wave can be derived for the diffraction of the #p-polarised beam [13].

We now turn to the analysis of the photoprocess dynamics in a thin polymer layer, ignoring for the moment the diffractional effects. Based on the results of this analysis, we will determine the parameters of the model amplitude-phase screens.

3. The dynamics of holographic recording in a polymer layer

We have previously shown [5] that, at the initial stage of irradiation by light ($t \ll b^{-1}$, where b is the rate of photoisomerisation), the principal role is the principal role is played by the processes in the azochromophore subsystem. For the recording light beams with arbitrary polarisation, the angular distribution density function of the azo-dye trans-isomers $n_1(\vartheta, \varphi, t)$ evolves according to the equation

$$\frac{\partial n_1(\vartheta,\varphi,t)}{\partial t} = -\frac{\gamma_1}{\hbar\omega}\, g\hat{\sigma}_1 : \boldsymbol{EE}\, n_1 + \left(\frac{1}{\tau} + \frac{\gamma_2}{\hbar\omega}\, g\hat{\sigma}_2 : \boldsymbol{EE}\right)$$
$$\times (N_0 - \langle n_1\rangle)\rho_0(\vartheta,\varphi). \quad (5)$$

Here $\boldsymbol{E} = \boldsymbol{E}_1 + \boldsymbol{E}_2$ is the total vector of the electric field of the light waves; γ_1 and γ_2 are the quantum yields of the trans-cis- and cis-trans-isomerisation processes, respectively; σ_1, σ_2 are the absorption tensors of the trans- and cis-isomers of the azo dye; ϑ, φ are the Euler angles defining the orientation of the selected trans-isomer of the azo dye; N_0 is the total concentration of the azo dye in the polymer; τ is the time of thermal relaxation of the cis-form to the trans-form; $g \equiv \bar{n}c_0/4\pi$ is a constant; $\bar{n}$ is the average refractive index of the polymer; c_0 is the speed of light in vacuum.

In this notations, the rate of photoisomerisation is given by $b = \gamma_1\sigma_1 I/\hbar\omega$, where I is the light intensity. The factor $\rho_0(\vartheta, \varphi)$ in the right-hand side of Eqn (5) accounts for the influence of the LC alignment on angular redistribution of the azo-dye trans-isomers during cis-trans-photoisomerisation. In the following we will assume that $\rho_0(\vartheta, \varphi)$ is determined by the Meyer – Saupe theory of self-consistent field and will use the approximation presented in Ref. [14]. We also assume that initially the polymer contains only trans-isomers that are distributed according to $\rho_0(\vartheta, \varphi)$:

$$n_1(\vartheta,\varphi,t=0) = N_0\rho_0(\vartheta,\varphi) \approx N_0[1 + 5SP_2(\boldsymbol{vm})]/4\pi, \quad (6)$$

where the vector $\boldsymbol{v} = \{0, \sin\xi, \cos\xi\}$ is the nematic director; $\boldsymbol{m} = \{\sin\vartheta\cos\varphi, \sin\vartheta\sin\varphi, \cos\vartheta\}$ is the unit vector determining the angular position of the chromophore trans-isomer; S is the orientation order parameter; and $P_2(x)$ is the second-order Legendre polynomial. To find $n_1(\vartheta, \varphi, t)$, we supplement Eqn (5) by the equations describing absorption of the light beams during their propagation in the polymer. Introducing the notation $I_i = gA_i^2/2$ ($i = 1, 2$ is the beam numbers) and using expressions from Ref. [5], we obtain

$$\frac{dI_i(z,x,t)}{dz} = -[\langle\hat{\sigma}_1 : \boldsymbol{e}_i\boldsymbol{e}_i\rangle_{n_1} + (N_0 - \langle n_1\rangle)\hat{\sigma}_2 : \boldsymbol{e}_i\boldsymbol{e}_i]I_i(z,x,t). \quad (7)$$

The averaging here is performed over the distribution $n_1(\vartheta, \varphi, t)$, and the boundary conditions for Eqn (7) are given by the intensity of the light beams at the input side of the layer, $I_i(z = 0, x, t)$. The simultaneous solution of Eqns (5) and (7) provides $n_1(\vartheta, \varphi, t)$, allowing one to find the light-induced changes Δn_{ind} in the refractive index of the current polymer layer. For example, the expression for the variation in the refractive index in the Y direction will take in accordance with Ref. [5] the following form

$$\Delta n_{ind}^y = 4\pi\{f\alpha_1 + \alpha_2[N_0 - \langle n_1(\vartheta,\varphi,t)\rangle]\}/2\bar{n},$$
$$f = \langle\sin^2\vartheta\sin^2\varphi\rangle_{n_1(\vartheta,\varphi,t)} - \langle\sin^2\vartheta\sin^2\varphi\rangle_{n_1(\vartheta,\varphi,t=0)}. \quad (8)$$

Here, α_1 and α_2 are the polarisabilities of the trans- and cis-isomers of the azo dye, respectively.

Note that the right-hand sides of Eqns (5) and (7) contain the products of the fast-oscillating spatial factors $\sim\exp(i\boldsymbol{k}_1\boldsymbol{r})$, $\exp(i\boldsymbol{k}_2\boldsymbol{r})$. Therefore, when analysing these equations, we will perform the averaging over the spatial frequencies k_1 and k_2

retaining only the interference terms of the form $\sim \cos(\boldsymbol{Kr})$ etc. Here, $\boldsymbol{K} \equiv \boldsymbol{k}_1 - \boldsymbol{k}_2$ is the vector of the spatial grating of the intensity distribution; $K = \left[k_1^2 + k_2^2 - 2k_1k_2\cos(\beta_1+\beta_2)\right]^{1/2}$. Due to saturation effects, the final expression for $n_1(\vartheta, \varphi, t)$, derived by the simultaneous solution of Eqns (5) and (7), is a nonlinear function of the amplitude of the interaction fields that contains the interference terms of the form $\sim \cos(m\boldsymbol{Kr})$. The produced grating of the refractive index is thus anharmonic.

The temporal dynamics of the light-induced processes in the polymer makes it necessary to retain the information about the local values of $\Delta\hat{n}(z, x, t)$, $\hat{T}(z, x, t)$ during the numerical solution of Eqns (5) and (7) so that this information can be used to calculate $\Delta\hat{n}(z, x, t+\Delta t)$, $\hat{T}(z, x, t+\Delta t)$ at the subsequent time instants. It turns out that in our case we can significantly reduce the amount of the intermediate data by converting in equation (5) to a new independent variable-the light exposure

$$W(z, x, t) = \int_0^t I(z, x, t')\mathrm{d}t',$$

where t is the current time. In this case, it is sufficient to retain the distribution of $W(z, x, t)$ over the entire polymer layer at the preceding computational step. Note that the passage to $W(z, x, t)$ in Eqn (5) is approximate and requires the validity of the inequality $I(z, x, t) \gg \hbar\omega/(\gamma_2\sigma_2\tau)$.

4. Holographic recording by s – s-polarised beams

The geometry of the holographic recording by s – s-polarised light beams is shown in Fig. 1a. In this case, the polarisation vectors of the electric field of the light waves satisfy $\boldsymbol{e}_1 = \boldsymbol{e}_2 = \boldsymbol{e}_y$. Introducing the notation $I(z, x, t) = I_1 + I_2 + 2(I_1I_2)^{1/2}\cos(Kx)$, where $K = 4\pi n_\perp \sin(\beta_1)\,\lambda_r^{-1}$ and $\beta_1 = \beta_2$ (the experimental condition), we rewrite Eqn (5) in the form

$$\frac{\partial n_1}{\partial t} = -\frac{\gamma_1\sigma_1 I(z, x, t)}{\hbar\omega}\, n_1 \sin^2\vartheta \sin^2\varphi + \left(\frac{1}{\tau} + \frac{\gamma_2\sigma_2 I(z, x, t)}{\hbar\omega}\right)(N_0 - \langle n_1\rangle)\rho_0(\vartheta, \varphi). \tag{9}$$

Taking into account the symmetry of the interaction, we can express the equation describing the light absorption in the polymer in terms of $I(z, x, t)$:

$$\frac{\mathrm{d}I(z, x, t)}{\mathrm{d}z} = -\left[\sigma_1\langle \sin^2\vartheta \sin^2\varphi\rangle_{n_1} + \sigma_2(N_0 - \langle n_1\rangle)\right] I(z, x, t). \tag{10}$$

Since expressions (9) and (10) are not explicitly dependent on x (they depend on x only through the boundary condition), the results of Ref. [5], derived for a single beam propagating in the polymer film, can be directly applied to solving Eqns (9) and (10). The light-induced addition to the refractive index $\Delta n_{\mathrm{ind}}^y$ and the transmission coefficient $T(z, x, t)$ of the current polymer layer are then determined by

$$\Delta n_{\mathrm{ind}}^y(z, x, t) = F[I(z, x, t), t, E_a],$$
$$T(x, z, t) \equiv \frac{I(z+\Delta z, x, t)}{I(z, x, t)} = \frac{G[I(z, x, t), \Delta z, t]}{I(z, x, t)}. \tag{11}$$

The explicit form of the functions G, F is given in Ref. [5].

Thus, if we have calculated the light intensity in the current point of the polymer layer according to Eqn (11), we can find $\Delta n_{\mathrm{ind}}^y$ in the same point at the next time instant. This procedure for calculating $\Delta n_{\mathrm{ind}}^y(z, x, t)$ and the transmission coefficient $T(z, x, t)$ will be later used to compute the parameters of the amplitude-phase screens during the numerical simulation according to the BPM scheme.

5. Holographic recording by s – p-polarised beams

The geometry of holographic recording by s-p-polarised light beams is shown in Fig. 1d. In the chosen system of coordinates, the unit vectors of the polarisation of the light beams are given by $\boldsymbol{e}_1 = \boldsymbol{e}_y$ and $\boldsymbol{e}_2 = \boldsymbol{e}_x\cos\beta_2 + \boldsymbol{e}_z\sin\beta_2$. In this case, we cannot rewrite Eqns (5) and (7) in terms of a single function of the two unknown intensities of the interacting light beams $I_{1,2}(z, x, t)$ as we did it before. Keeping the general form of Eqns (5) and (7), we therefore obtain

$$\frac{\partial n_1}{\partial t} = -\frac{\gamma_1\sigma_1}{\hbar\omega}\left\{B_1(\vartheta, \varphi)I_1 + B_2(\vartheta, \varphi)I_2 + 2[B_1(\vartheta, \varphi)B_2(\vartheta, \varphi)I_1I_2]^{1/2}\cos(Kx)\right\} n_1 + \left[\frac{1}{\tau} + \frac{\gamma_2\sigma_2}{\hbar\omega}(I_1 + I_2)\right](N_0 - \langle n_1\rangle)\rho_0(\vartheta, \varphi), \tag{12}$$

$$\frac{\mathrm{d}I_i(z, x, t)}{\mathrm{d}z} = -[\sigma_1\langle B_i(\vartheta, \varphi)\rangle_{n_1} + \sigma_2(N_0 - \langle n_1\rangle)I_i(z, x, t). \tag{13}$$

Here, $i = 1, 2$ is the beam numbers;

$$B_1(\vartheta, \varphi) = \sin^2\vartheta\sin^2\varphi,$$
$$B_2(\vartheta, \varphi) = (\sin\beta_2\cos\vartheta + \cos\beta_2\sin\vartheta\cos\varphi)^2 \tag{14}$$

are the angular coefficients determined by the projections of the trans-isomer principal axes on the electric field vectors of the light beams. In a close analogy with Ref. [5], the solution of Eqn (12) can be found as a power series with respect to the small parameter bt ($bt \ll 1$) using the method of successive approximations. Retaining the second-order terms with respect to bt and grouping the coefficients before equal powers of the beam intensities, we derive

$$n_1(\vartheta, \varphi, t) = N_0\rho_0(\vartheta, \varphi) + \sum_{i=1}^{2}\sum_{j=0}^{2i} K_i^j(\vartheta, \varphi, t) \times [I_1(z, x, t)]^{j/2}[I_2(z, x, t)]^{i-j/2}. \tag{15}$$

Here the coefficients $K_i^j(\vartheta, \varphi, t)$ depend on angles and time; they can be determined by substituting Eqn (15) into Eqn (12). Then, we use the derived Eqn (15) to calculate the averages in the right-hand side of Eqn (13):

$$\frac{\mathrm{d}I_1(z, x, t)}{\mathrm{d}z} = -C_1^1I_1 + C_2^1(I_1)^{3/2}(I_2)^{1/2} + C_3^1I_1I_2,$$
$$\frac{\mathrm{d}I_2(z, x, t)}{\mathrm{d}z} = -C_1^2I_2 + C_2^2(I_2)^{3/2}(I_1)^{1/2} + C_3^2I_2I_1. \tag{16}$$

To simplify the notation in system (16), we introduce the coefficients C_q^l ($l = 1, 2$ is the beam number) that result from averaging $B_i(\vartheta, \varphi)$ over the distribution (15). Simultaneous Eqns (16) allow one to determine the transmission coefficients of the selected polymer layer for the recording light beams. When solving this system of equations numerically, we calculated the new intensities $I_{1,2}(z + \Delta z, x, t)$ using the Runge – Kutta method that provides the fourth-order accuracy with respect to the step Δz. Substituting the solution of system (16) $I_{1,2}(z, x, t)$ into extension (15), we derive the final expression for $n_1(\vartheta, \varphi, t)$ that takes into account attenuation of the intensity along the axis Z. The expression for Δn_{ind}^y in the direction of the vector $\boldsymbol{E}_{\text{p}}$ (corresponding to intra-modal hologram read-out) can be found using Eqn (8). Since the complete expressions are rather cumbersome, we do not present them here.

We now proceed to the description of the experiments and comparison of the experimental data with the results of the numerical simulation.

6. The experiment. Comparison with the results of the numerical simulation

We carried out the holographic recording experiments using film samples of side-chain nematic LC polymers with the molar concentration of chemically bound azo-dye fragments [10,11] equal to 20 %. The nematic phase of the polymer sample existed in the temperature range 40 – 104°C. For the experiments, a cell was prepared containing a polymer layer $L = 50$ μm thick sandwiched between two glass plates with transparent conductive SnO_2 electrodes. The initially incomplete planar alignment of the polymer film was achieved by rubbing the surfaces of the limiting plates. We applied to the conductive coatings of the glass plates an alternate voltage $U_{\text{a}} = 0 - 100$ V at a frequency of 350 Hz, which allowed us to change the orientation of the nematic director in the polymer layer (due to alignment of the mesogenic fragments along the field). The cell design also included the capability to increase and stabilise the working temperature of the polymer film in the interval 40 – 120°C with an accuracy of 0.1°C.

The goniometric measurements of the cell revealed the principal values of the refractive index of the homotropically aligned polymer layer: $n_{||} \approx 1.78$, $n_{\perp} \approx 1.46$ (for $U_{\text{a}} = 80$ V), which is in a good agreement with the values found in Ref. [11] for similar media. The optical densities of the film for $\lambda_{\text{r}} \approx$ 532 nm and $\lambda_{\text{p}} \approx 633$ nm in the longitudinal and transverse directions with respect to the preferred director orientation amounted respectively to $D_{\perp} \approx 0.9, D_{||} \approx 2.8$ and $D_{\perp} \approx 0.07$, $D_{||} \approx 0.2$.

The hologram was recorded in the polymer sample by the second harmonic of an LTN-402A Nd : YAG laser ($\lambda_{\text{r}} \approx 532$ nm) using the transmission interference scheme. Fig. 2 shows the schematic overview of the setup. The laser beam passed through the electromechanical shutter *1* and the collimator *2* with the aperture of 20 μm, and finally impinged on the beamsplitter *3*. The resulting light beams were reflected by the mirrors *6* and *7* and interfered in the plane of the polymer film *11*. The double Fresnel rhombs *4* and *5* defined the polarisation of the beams, and a set of neutral density filters *8* was used to equalise the beam intensities.

The hologram read-out was simultaneous with their recording. It was realised by the radiation of a LGN-207A He – Ne laser ($\lambda_{\text{p}} \approx 633$ nm) propagating at the angle ψ_1 (in the air) with respect to the polymer film normal. Photodetector *9* measured the intensity of light in the Bragg diffractional order I_{B}, allowing us to determine the diffractional efficiency $\eta(t) = I_{\text{B}}/I_{\text{p}}$, where I_{p} is the intensity of the probe beam. We calculated $\eta(t)$ only for the polymer layer; the influence of the glass plates of the cell was taken into account during the data processing. Photodetector *10* was used for auxiliary goniometric measurements. The general control of the experimental setup and the data acquisition was performed using a personal computer connected

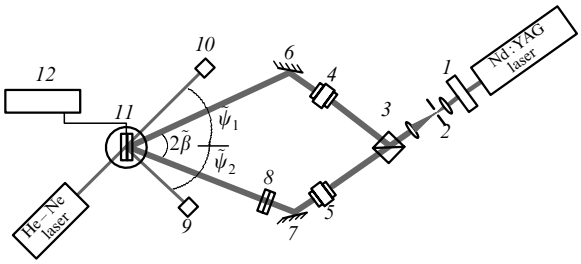

Figure 2. Schematic of the experimental setup.

via the electronic control unit *12* and a DAC/ADC board.

The recording light beams, which were converging in the air at the angle $2\tilde{\beta} \approx 28°$, created a grating with the spatial frequency Λ^{-1} of approximately 909 lines mm^{-1} (it was approximately the same for the cases shown in Figs 1a and d). The read-out angle $\tilde{\psi}_1 \approx 16.5°$, satisfying the Bragg condition for the geometry of Fig. 1 a, was determined experimentally at an orienting voltage of 40 V (350 Hz). For the geometry of Fig. 1 d, the angle was $\tilde{\psi}_1 \approx 17.5°$ at the same voltage. During the experiments the read-out angles were kept constant.

The curves in Fig. 3 show the dynamics of the diffraction efficiency for various applied voltages and polarisations of the recording beams. The hologram was recorded by two light beams of equal intensity ($I_1 \approx I_2 \approx 85$ mW cm^{-2}); the temperature of the sample was ~70°C. One can see from Fig. 3 a, that, in the geometry of Fig. 1 a, an increase in the strength of the orienting electric field leads to an increase in the maximum value of $\eta(t)$. This can be explained by the fact that in a stronger field the homotropical alignment of the polar groups leads to a reduction in the light absorption ($\lambda_{\text{r}} \approx 532$ nm) of the polymer; as a result, the effective depth of the hologram recording increases.

In the geometry of Fig. 1 d, we observe the inverse dependence: $\eta(t)$ decreases with increasing field strength (see the curves in Fig. 3 b). In this case, a stronger field leads to a reduction in the nondiagonal elements of the tensor $\Delta\hat{n}(z, x, t)$ at the grating frequency, which are responsible for the intermodal diffractional processes. The curves representing the simulation results were calculated for the same conditions as in the experiments. The parameters of the polymer were the same as in Ref. [5]. One can see that, in the region $t \ll b^{-1}$ (in our case, $b^{-1} \approx 9$ s), the theoretical curves are in good agreement with the experimental data.

7. Conclusions

We have investigated experimentally the features of hologram recording in a film of azo-containing nematic polymer in the presence of orienting electric field. The possibility was demonstrated to efficiently control the holographic charac-

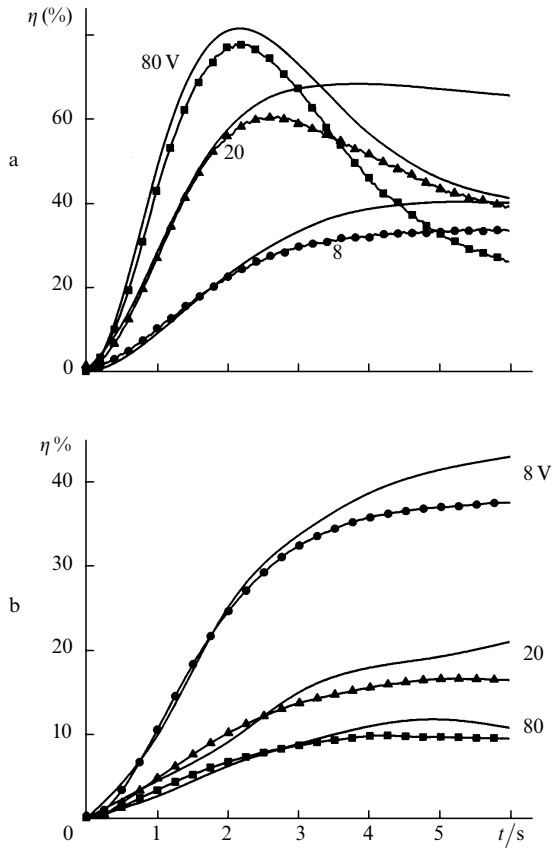

Figure 3. Dynamics of the diffraction efficiency of the holograms in the nematic polymer film in the presence of the orienting electric field for the recording by s – s-polarised a and s – p-polarised b beams. The solid curves represent the simulation results; the symbols represent the experimental points.

teristics of the polymer layer by varying the strength of the applied field. We developed a theoretical model that took into account the anisotropic properties of the compound and therefore adequately described the dynamics of the holographic properties that was based on the intra-modal and the intermodal diffraction. The obtained theoretical results were in good agreement with the experimental data.

Acknowledgements. The authors thank S G Kostromin and A I Stakhanov for preparing the polymer samples, and V I Shmal'gauzen for useful discussions. This work was supported by the Russian Foundation for Basic Research (grant no. 98-02-17125) and INTAS (grant no. 97-1672).

References

1. Sutherland R L, Natarajan L V, Tondiglia V P, Bunning T J, Adams W W *Appl. Phys. Letts* **64** 1074 (1994)
2. Tondiglia V P, Natarajan L V, Sutherland R L, Bunning T J, Adams W W Optics Letts 20 1325 (1995)
3. Sutherland R L, Natarajan L V, Tondiglia V P, Bunning T J, Adams W W *Phoc. SPIE* **2352** 309 (1995)
4. Larichev A V, Simonov A N, Shibaev V P, Stakhanov A I in: *Polymer Preprints of Symposium on Azo-Containing Polymers* (ASC Annual Meeting, Boston, 1998, v. 39, p. 274)
5. Simonov A N, Larichev A V *Kvantovaya Elektron. (Moscow)* **28** 87 (1999) [*Quantum Electron.* **29** 644 (1999)]
6. Todorov T, Nikolova L, Tomova N *Appl. Optics* **23** 4588 (1984)
7. Pedersen T G, Johansen P M, Holme N C R, Ramanujam P S, Hvilsted S *Phys. Rev. Letts* **80** 89 (1998)
8. Huang T, Wagner K H *J. Opt. Soc. Am. B* **13** 282 (1996).
9. Petrov M P, Stepanov S I, Khomenko A V F*otorefraktivnye Kristally v Kogerentnoi Optike* [Photorefractive Crystals in Coherent Optics] (Nauka, St.Petersburg, 1992, Ch. 5).
10. Shibaev V P, Kostromin S G, Ivanov S A In: *Polymers As Electrooptical and Photooptical Active Media* (ed. V P Shibaev) (Springer-Verlag, Berlin, 1996, p. 37)
11. Shibaev V P, Kostromin S G, Ivanov S A *Vysokomol. Soedin. Ser. A* **39** 1 (1997)
12. Bridges R E, Boyd R W, Agrawal G P *J. Opt. Soc. Am. B* **13** 553 (1996)
13. Fleck J A, Feit M D *J. Opt. Soc. Am.* **73** 920 (1983)
14. Zolot'ko A S, Kitaeva V F, Terskov D B *Zh. Eksp. Teor. Fiz.* **106** 1722 (1994) [*JETP* **79** 931 (1994)].